Charmonium production in Pb–Pb interactions at 158 GeV/c per nucleon

Luciano Ramello for the NA50 Collaboration

M.C. Abreu[6,a], B. Alessandro[11], C. Alexa[3], R. Arnaldi[11], J. Astruc[8], M. Atayan[13], C. Baglin[1], A. Baldit[2], M. Bedjidian[12], F. Bellaiche[12], S. Beolè[11], V. Boldea[3], P. Bordalo[6,b], A. Bussière[1], V. Capony[1], L. Casagrande[6], J. Castor[2], T. Chambon[2], B. Chaurand[9], I. Chevrot[2], B. Cheynis[12], E. Chiavassa[11], C. Cicalò[4], M.P. Comets[8], S. Constantinescu[3], J. Cruz[6], A. De Falco[4] N. De Marco[11], G. Dellacasa[11,c], A. Devaux[2], S. Dita[3], O. Drapier[12], B. Espagnon[2], J. Fargeix[2], S.N. Filippov[7], F. Fleuret[9], P. Force[2], M. Gallio[11], Y.K. Gavrilov[7], C. Gerschel[8], P. Giubellino[11], M.B. Golubeva[7], M. Gonin[9], A.A. Grigorian[13], J.Y. Grossiord[12], F.F. Guber[7], A. Guichard[12], H. Gulkanyan[13], R. Hakobyan[13], R. Haroutunian[12], M. Idzik[11,d], D. Jouan[8], T.L. Karavitcheva[7], L. Kluberg[9], A.B. Kurepin[7], Y. Le Bornec[8], C. Lourenço[5], M. Mac Cormick[8], P. Macciotta[4], A. Marzari-Chiesa[11], M. Masera[11], A. Masoni[4], S. Mehrabyan[13], S. Mourgues[2], A. Musso[11], F. Ohlsson-Malek[12,e], P. Petiau[9], A. Piccotti[11], J.R. Pizzi[12], W.L. Prado da Silva[11,f], G. Puddu[4], C. Quintans[6], C. Racca[10], L. Ramello[11,c], S. Ramos[6,b], P. Rato-Mendes[11] L. Riccati[11], A. Romana[9], S. Sartori[11], P. Saturnini[2], E. Scomparin[5,g], S. Serci[4], R. Shahoyan[6,h], S. Silva[6], C. Soave[11], P. Sonderegger[5,b], X. Tarrago[8], P. Temnikov[4], N.S. Topilskaya[7], G.L. Usai[4], C. Vale[6], E. Vercellin[11], and N. Willis[8].

[1] LAPP, CNRS–IN2P3, Annecy–le–Vieux, France; [2] LPC, Université Blaise Pascal and CNRS–IN2P3, Aubière, France; [3] IFA, Bucharest, Romania; [4] Università di Cagliari and INFN, Cagliari, Italy; [5] CERN, Geneva, Switzerland; [6] LIP, Lisbon, Portugal; [7] INR, Moscow, Russia; [8] IPN, Université Paris–Sud and CNRS–IN2P3, Orsay, France; [9] LPNHE, Ecole Polytechnique and CNRS–IN2P3, Palaiseau, France; [10] IReS, Université Louis Pasteur and CNRS–IN2P3, Strasbourg, France; [11] Università di Torino and INFN, Torino, Italy; [12] IPN Lyon, Université Claude Bernard and CNRS–IN2P3, Villeurbanne, France; [13] YerPhI, Yerevan, Armenia.
[a] also at FCUL, Universitade de Lisboa, Lisbon, Portugal; [b] also at IST, Universitade Técnica de Lisboa, Lisbon, Portugal; [c] Dipartimento di Scienze e Tecnologie Avanzate, II Facoltà di Scienze, Alessandria, Italy; [d] now at Faculty of Physics and Nuclear Techniques, University of Mining and Metallurgy, Cracow, Poland; [e] now at ISN, Univ. Joseph Fourier and CNRS-IN2P3, Grenoble, France; [f] Now at UERJ, Rio de Janeiro, Brazil; [g] On leave of absence from INFN Torino, Italy; [h] On leave of absence from YerPhI, Yerevan, Armenia.

The NA50 collaboration has measured J/ψ, ψ' and Drell–Yan pair production in Pb–Pb interactions at 158 GeV/c per nucleon at the CERN SPS. Final results from the 1995 run and preliminary ones from the higher statistics 1996 run are presented.

An anomalous J/ψ suppression (relative to the Drell–Yan process) has been observed with respect to the suppression pattern established in experiments NA38 and NA51 with proton, oxygen and sulfur beams. The 1996 data allow a detailed study of the suppression pattern in the Pb–Pb sample itself, showing a discontinuity around an E_T value (the neutral transverse electromagnetic energy) of 50 GeV. The ψ' is also suppressed relative to Drell–Yan, with a pattern very similar to the one observed in S–U collisions. Finally, the p_T distributions of

dimuons are presented. The average p_T^2 of the J/ψ in Pb–Pb collisions does not increase any more with E_T above 100 GeV.

1. INTRODUCTION

The experimental study of matter at high energy density, triggered by the expectation of forming a quark–gluon plasma (QGP), has been pursued for more than a decade with the ultrarelativistic heavy ions beams available at the CERN SPS and the BNL AGS. Among the proposed signatures for the QGP, the suppression of charmonium states [1] by the Debye screening mechanism is particularly interesting: charmonium is formed by a hard process in the first stages of the collision, and its fate can be compared to that of Drell-Yan lepton pairs, which are unaffected by the QGP.

The NA38 collaboration, starting in 1986, has made an extensive study [2] of charmonium and Drell–Yan production with proton, oxygen and sulfur beams on several targets at the CERN SPS, using the dimuon spectrometer of experiment NA10, an active target and an electromagnetic calorimeter as an indicator of the centrality of the collision. A considerable amount of theoretical work on the NA38 results has led to the present widely accepted understanding of the J/ψ suppression observed there as being due to absorption in the nuclear medium.

This study has been extended to Pb–Pb collisions by the NA50 collaboration, which has performed a major upgrade of the beam detector, of the active target system and of the centrality detectors, as presented in section 2, which also illustrates the analysis procedure. After a first setting–up run in late 1994, NA50 has collected data in autumn 1995 and, with higher integrated luminosity, in autumn 1996.

Preliminary results from the 1995 charmonium analysis were presented at the Quark Matter '96 conference [3]; final results from 1995 have been very recently published [4,5] and are summarised briefly in this paper in section 3.

New results on J/ψ, ψ' and Drell–Yan production from the the high statistics 1996 run are presented in section 4. A preliminary version of the 1996 analysis has been presented previously [6,7]. In this paper an updated version, although still preliminary, is presented.

In addition to the high mass region (J/ψ, ψ' and Drell–Yan), which is the subject of this paper, also the ρ, ω and ϕ vector mesons [8] and the intermediate and low mass continua [9] are being investigated.

2. EXPERIMENTAL METHOD

2.1. Apparatus and data taking conditions

The NA50 apparatus consists of a muon spectrometer complemented by detectors to define the incoming beam, recognize interactions in the target, and measure the centrality of the nucleus–nucleus collision. Because of the small production cross section of the charmonium resonances and of their small branching ratios to $\mu^+\mu^-$ pairs, high integrated luminosity is required. A segmented active target is used to reject events contaminated by beam fragment or secondary particle reinteractions.

The experiment's layout is shown in figure 1, and the detail of the target region, with the active target and the centrality detectors, is shown in figure 2.

The magnetic spectrometer consists of a hadron absorber, an air core toroidal magnet,

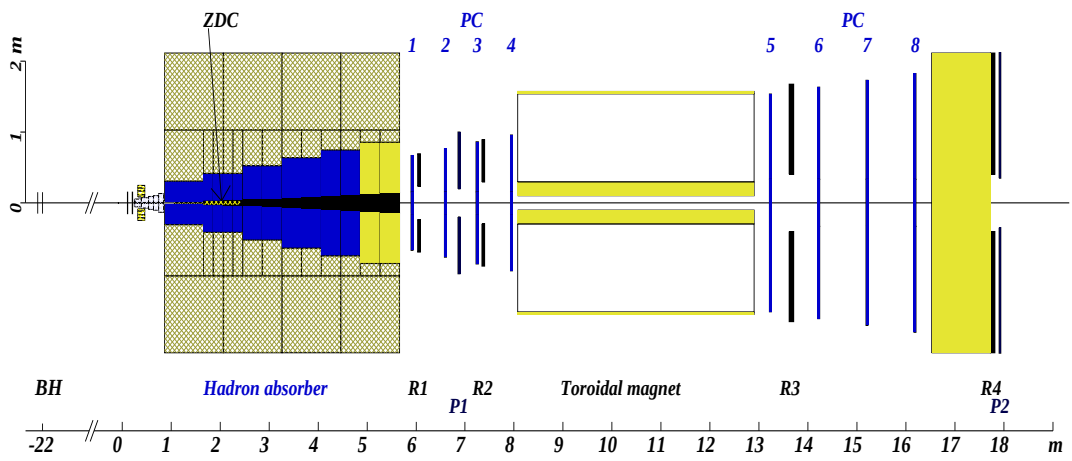

Figure 1. The NA50 apparatus.

8 MWPCs (PC1–PC8) and 6 scintillator hodoscopes (R1–R4 and P1,P2) for triggering purposes; the last hodoscope R4 is preceded by an iron wall to suppress hadronic punch–through. To reduce the amount of combinatorial background from independent decays of π and K mesons while keeping a good resolution on the invariant mass of the dimuon, the last target is located only 15 cm upstream from the absorber which is made of a 60 cm section of BeO followed by 400 cm of carbon and then by 80 cm of iron. Muons are detected with good acceptance in the rapidity interval $2.92 \leq y_{lab} \leq 3.92$ (corresponding to $0 \leq y_{cm} \leq 1$), with a mass resolution of 3.2% at the J/ψ.

The event centrality is estimated using three independent detectors: the Pb–scintillating fibers electromagnetic calorimeter EMC ($1.1 \leq \eta_{lab} \leq 2.3$, subdivided in 6 azimuthal sectors and 4 rings), measuring the neutral transverse energy produced in the interaction; the Tantalum–quartz fibers zero degree calorimeter ZDC ($\eta_{lab} \geq 6.2$), measuring the energy of non–interacting beam fragments, and the 2–plane, high–granularity silicon strip multiplicity detector MD ($1.5 \leq \eta_{lab} \leq 3.5$ is the full coverage, achieved in the 1996 run), measuring the charged particle multiplicity.

The incident Pb ions are counted by a 16–segment quartz beam hodoscope BH (located far upstream where the beam transverse dimension is large) which is also used to reject beam pile–up. The active target is made of 7 Pb subtargets with vertex identification provided by quartz Cherenkov counters, in order both to improve the dimuon invariant mass resolution and to reject reinteractions of beam fragments. In 1995, the subtargets were 1 mm thick leading to a total of 19% of an interaction length for Pb; in 1996, the thickness was increased to 2 mm for five of them leading to 32% of an interaction length.

In 1995, at an average beam intensity of 3.2×10^7 Pb ions per burst, about 58×10^6 dimuon triggers were collected, giving $\approx 50,000 J/\psi$ events at the end of the analysis. In

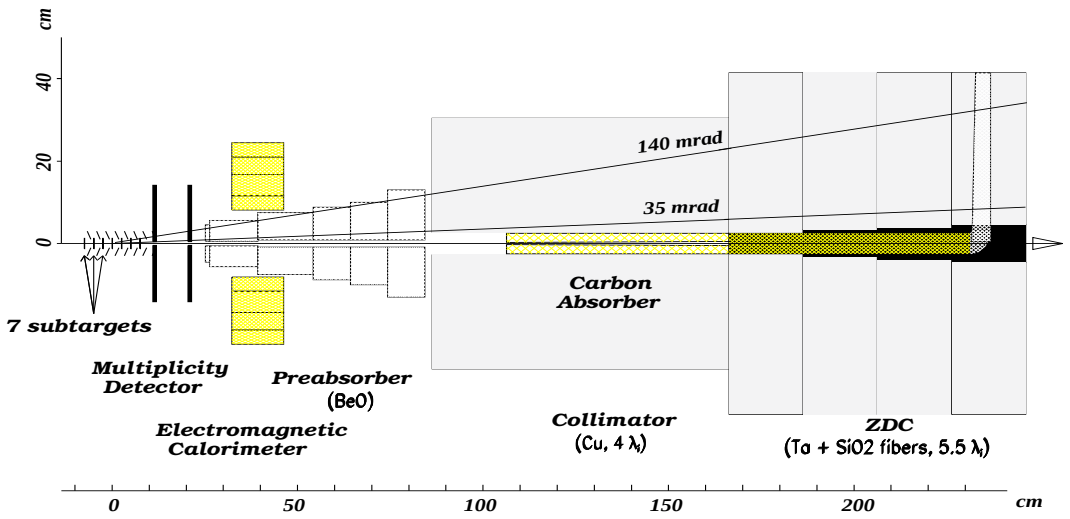

Figure 2. The NA50 target region, including the Active Target, the Multiplicity Detector, the Electromagnetic Calorimeter and the Zero Degree Calorimeter.

1996 the intensity was increased to 5.4×10^7 Pb ions per burst, and the beam quality was improved, reducing the out–of–target background: in this way, about 170×10^6 triggers were collected, leading to $\approx 250,000 J/\psi$ events.

2.2. Analysis

Triggered events are retained for analysis if only one incident ion is detected in the Beam Hodoscope, no interaction is occurring in the BH itself, no signal is present in the halo counters and if the event is identified as having taken place in the target (this identification is further discussed in the following). In addition, it is required that two and only two muon tracks are in the fiducial region of the spectrometer (which excludes the six coils of the toroidal magnet), and that they would both be accepted if they had been of the opposite charge (in order to have the same acceptance of the spectrometer for any charge state of the dimuon).

The standard method to identify an interaction in the target (and the only method used for the 1995 data sample) requires a positive subtarget identification by the Cherenkov counter system. However this method becomes inefficient for peripheral interactions, and more so in 1996 due to increased noise from secondary electrons (delta rays) ejected by the Pb ion when crossing the thicker subtargets.

Thanks to better beam conditions in 1996, it has been possible to base the interaction identification on a contour cut on the E_T–E_{ZDC} correlation [6] at the 2σ level. Figure 3 shows such a correlation for the Cherenkov counter identification method (left) and the contour cut one (right). Most peripheral interactions are clearly lost with the first method.

Most peripheral events retained by the contour cut have no subtarget assignment, hence they have a slightly worse mass resolution (about 8% increase at the J/ψ).

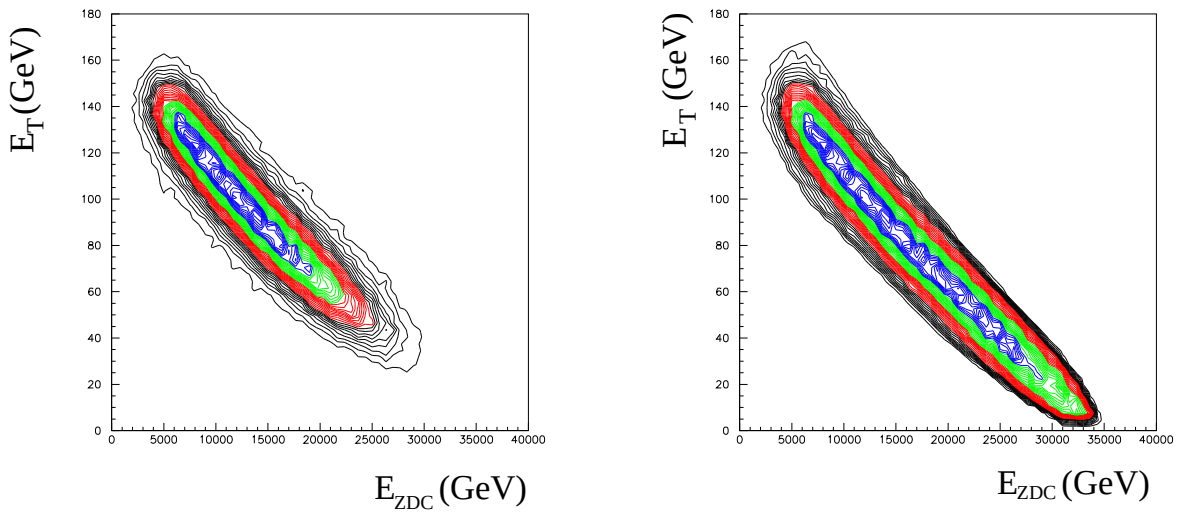

Figure 3. The E_T–E_{ZDC} correlation of identified interactions when the Cherenkov counter identification (left) or the contour cut (right) is used (1996 data).

An independent subtarget algorithm has been developed using the two planes of the multiplicity detector (MD) in coincidence; this new algorithm shows better efficiency for peripheral events, as shown in fig. 4, where the number of triggers identified by the E_T–E_{ZDC} contour cut, by the Cherenkov counter method and by the MD method are displayed as a function of E_T. The multiplicity detector identification is essentially equivalent to the contour cut one, with the advantage of a positive subtarget identification; however, the MD data processing being still incomplete, the contour cut has been used in the analysis presented in section 4.

An additional severe cut on the distance between each muon track and the beam axis has been applied to the 1996 data sample, in order to reduce the background from non–target interactions. This background is present when the E_T–E_{ZDC} contour cut method alone is used for the interaction identification.

The dimuon kinematical domain is defined by $0 \leq y_{cm} \leq 1$ (y_{cm} = center of mass dimuon rapidity) and $-0.5 \leq cos(\theta_{CS}) \leq 0.5$ (θ_{CS} = muon polar angle in the Collins–Soper frame), where the acceptance of the spectrometer is at least 10% of its maximum. The acceptance of the spectrometer for the 1995 and 1996 sets of kinematical cuts is given in table 1 for J/ψ, ψ' and Drell–Yan.

The invariant mass spectrum for opposite sign dimuons is shown in fig. 5, for the 1995 data sample. The contribution from two muons originating from uncorrelated π and K decays is evaluated with a standard procedure using the two like-sign samples of muon pairs. The signal-to-background ratio is larger than 10 at the J/ψ peak. The mass spectrum is fitted as the superposition of five contributions: J/ψ, ψ', Drell–Yan,

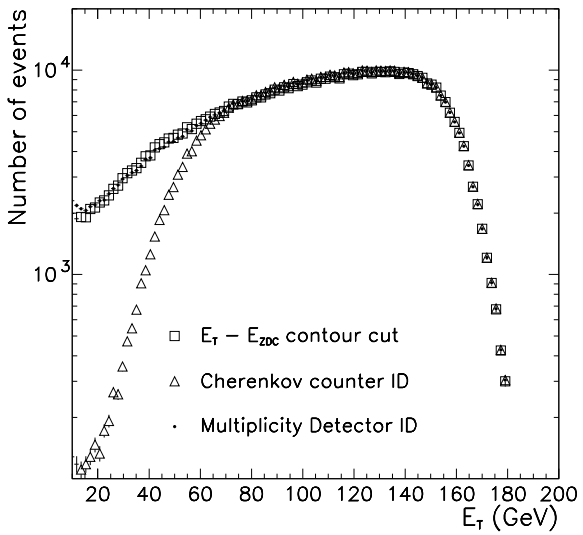

Figure 4. The E_T spectra of events accepted by different interaction identification methods.

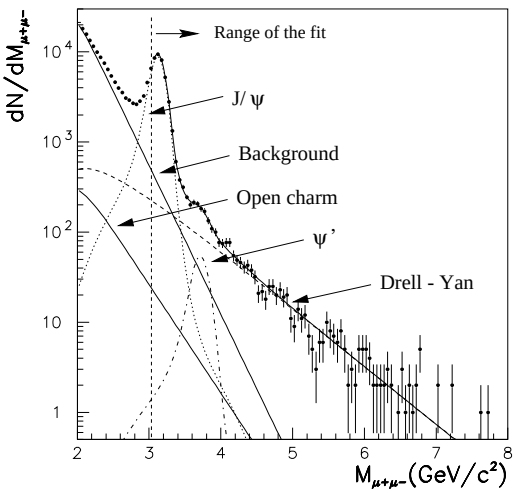

Figure 5. Opposite–sign dimuon mass distribution with superimposed fit.

Table 1
Spectrometer acceptances

Sample	J/ψ	ψ'	$DY\,(2.9-4.5)$
1995	13.5%	16.1%	15.1%
1996	7.5%	8.9%	8.4%

open charm semileptonic decays including a charm-like excess in the intermediate mass region [9,10] and background:

$$\frac{dN^{+-}}{dM} = A_{J/\psi} \cdot \frac{dN^{J/\psi}}{dM} + A_{\psi'} \cdot \frac{dN^{\psi'}}{dM} + A_{DY} \cdot \frac{dN^{DY}}{dM} + \frac{dN^{D\overline{D}}}{dM} + \frac{dN^{bg}}{dM} \qquad (1)$$

The line shapes are determined via the NA50 MonteCarlo program followed by the standard reconstruction program, thus including the effects of momentum resolution in the spectrometer and multiple scattering and energy loss in the absorber.

The final fit is performed above a lower limit of 3.05 GeV/c^2 with five free parameters: $A_{J/\psi}$, $A_{\psi'}$, A_{DY}, and the mass and width of the gaussian line shape of the J/ψ (charm and background are constrained by previous fits). Mass and width of the ψ' are linked to those of the J/ψ. The 1995 sample is usually analysed in 5 centrality bins, while the 1996 one is analysed in up to 15 bins, thanks to the higher statistics.

To verify the sensitivity of results either to the choice of line shapes used in the fits or to the detailed fit procedure, in some cases the raw numbers of events in the J/ψ peak

and the Drell–Yan events above 4.2 GeV/c^2 (practically free from other contributions) have been compared to the fitted values (see section 4).

3. RESULTS FROM THE 1995 RUN

The final results on J/ψ and Drell–Yan production from the 1995 data, which have been recently published [4,5], are summarised here.

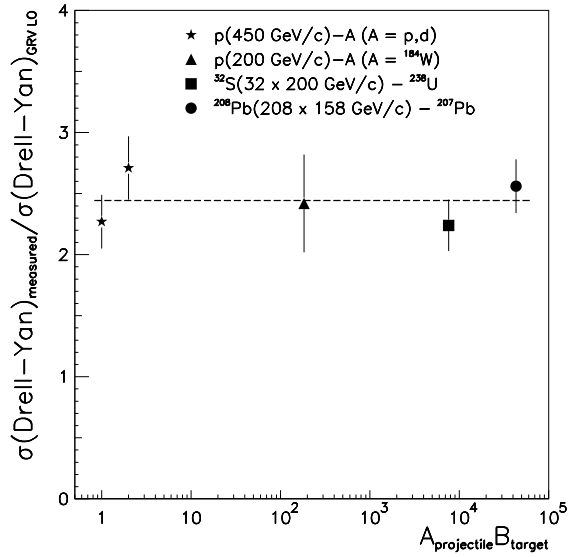

Figure 6. The Drell–Yan K–ratio vs. AB for different systems.

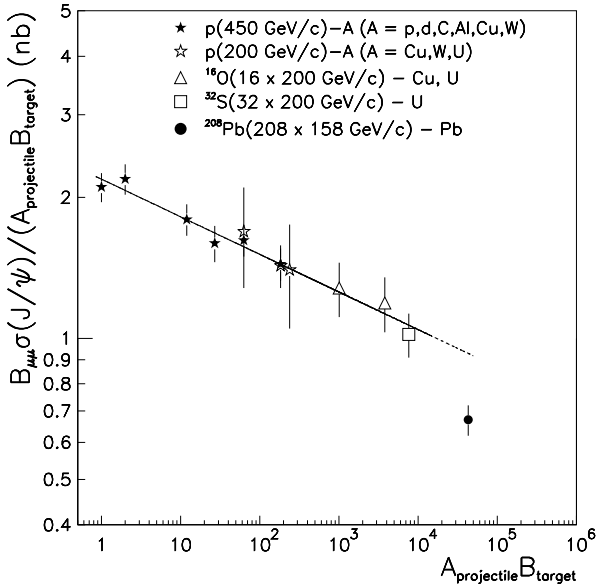

Figure 7. The J/ψ cross–section vs. AB for different systems (Pb: 1995 data).

The nuclear dependence of the production cross–section for hard processes is usually parametrised as

$$\sigma^{AB} = \sigma^{NN}(AB)^{\alpha} \tag{2}$$

with A projectile and B target nucleons. For the Drell–Yan process, previous NA38 measurements at 200 GeV/c per nucleon and NA51 p–p, p–d measurements [11] at 450 GeV/c are consistent with a value $\alpha = 1$, indicating that no nuclear absorption is taking place.

In Pb–Pb we measure $\sigma_{DY}^{2.9-8.0} = 1.49 \pm 0.02 \pm 0.11$ μb at 158 GeV/c per nucleon. To compare with NA38 and NA51 we have to rescale data at the same beam momentum (200 GeV/c) and to apply an isospin correction to refer all data to p–p collisions:

$$\sigma_{DY}^{AB}(corr.) = \sigma_{DY}^{AB}(meas.) \times \frac{AB\sigma_{DY}^{pp}(LO)}{\sigma_{DY}^{AB}(LO)} \tag{3}$$

where we have used the GRV LO (leading order) set of nucleon structure functions [12]. The rescaled Pb–Pb cross–section is found to compatible with $\alpha = 1$ (a fit including Pb–Pb gives $\alpha = 1.002 \pm 0.001$), a fact which is reflected in fig. 6, which shows that the so–called Drell–Yan K–factor (ratio of measured to leading–order calculated cross–section) is indeed constant as a function of AB.

The scaling of J/ψ cross–section with AB as measured by NA38 and NA51 (at 200 GeV/c and 450 GeV/c, resp.) is also well described by expression (3) from proton–proton up to sulfur–uranium collisions, with $\alpha = 0.92 \pm 0.015$, as shown in fig. 7. This value is also compatible with the one obtained by the FNAL experiment E772 at higher beam momentum [13]. These results indicate a nuclear effect which has been interpreted as absorption of the pre–resonant $c\overline{c}$ state in nuclear matter, and is normally called "standard" J/ψ suppression (see for example in [14]).

The cross–section measured in Pb–Pb collisions is $B_{\mu\mu}\sigma_{J/\psi} = 21.9 \pm 0.2 \pm 1.6$ μb at 158 GeV/c. Again, to compare to NA38 and NA51, this value has been rescaled to 200 GeV/c using the Schuler parametrisation [15]. The rescaled value, also shown in fig. 7, is significantly lower, a factor 0.74 ± 0.04, than the absorption fit line. This result suggests a new mechanism responsible for what has been termed "anomalous J/ψ suppression" [5].

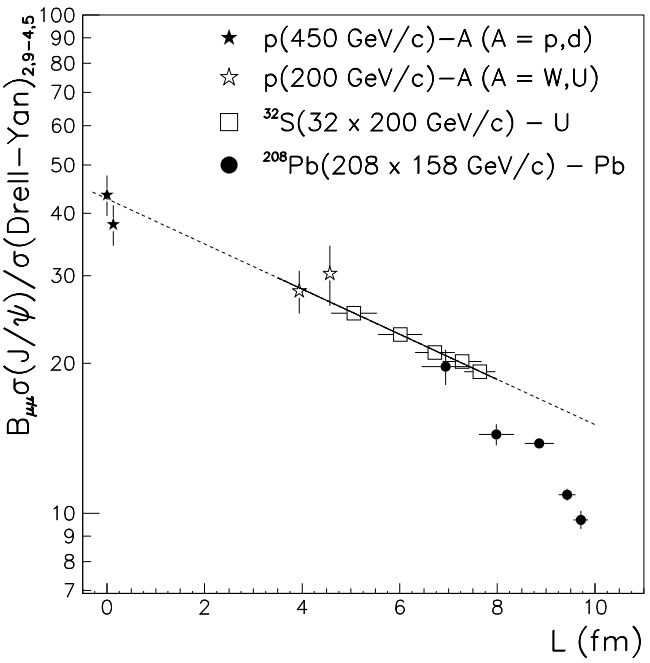

Figure 8. The ratio $(J/\psi)/DY$ vs. L at 200 GeV/c (1995 data).

To investigate further charmonium production, we will use the Drell–Yan cross–section

as a measurement of the number of collisions (since it scales like AB): the ratio $B_{\mu\mu}\sigma^{J/\psi}/\sigma^{DY}$ is free from luminosity normalisation errors (the systematic error, which is of 7% on absolute cross–sections, drops to 1.5% on the ratio). This ratio can be studied as a function of the transverse energy E_T which is a measurement of centrality in a given system. All Drell–Yan cross–sections used in ratios will be referred to the mass interval 2.9–4.5 GeV/c^2.

To compare different systems, characterised by different kinematics and in some cases also different experimental E_T coverage, a new variable is needed: this is L, defined as the geometrical mean path length of the produced $c\overline{c}$ state through nuclear matter. We compute L via a MonteCarlo program which, for a given impact parameter b, performs a weighted average over the possible production points:

$$\overline{L}(b) = \frac{1}{\rho_0}\langle \rho L \rangle$$

using a standard Woods–Saxon nuclear density function ρ; L is computed as the sum of the residual paths through projectile and target nucleus, $L = L_p + L_t$.

The relation between E_T and the impact parameter b is obtained via a MonteCarlo calculation which is adjusted for each system to the observed dN/dE_T distribution for high–mass Drell–Yan events; using the $\overline{L}(b)$ relation we can then estimate the average L of each transverse energy class, in a way which is essentially independent on the precise knowledge of the absolute E_T scale. More details of the method can be found in [4,5].

The NA38 data on the ratio $B_{\mu\mu}\sigma^{J/\psi}/\sigma^{DY}$, for those systems where statistically significant Drell–Yan data exist, are reported as a function of L in fig. 8, together with the Pb–Pb 1995 data rescaled to 200 GeV/c and subdivided in five E_T classes. A good fit to p–W, p–U and S–U data is obtained with the absorption model

$$\frac{B\sigma_{J/\psi}}{\sigma_{DY}} = \exp(-\rho\sigma_{abs}L) \qquad (4)$$

for an absorption cross–section $\sigma_{abs} = 6.2 \pm 0.7$ mb. This fit is also in agreement with p–p and p–d NA51 data [11] rescaled to 200 GeV/c.

While the most peripheral Pb–Pb point essentially agrees with the absorption model, the points at $L > 7.5$ fm are strongly suppressed, by factors ranging between 0.81 ± 0.03 and 0.62 ± 0.04. This striking result motivated us to collect a much larger sample in the 1996 run, whose preliminary results are presented in the next section.

4. NEW RESULTS FROM THE 1996 RUN

When comparing the following 1996 Pb–Pb results to other systems, we decided (i) to refer all data to 158 GeV/c, and (ii) to adopt for the Drell–Yan isospin correction the nucleon structure function set "MRS 43" (set A of ref. [16]) which does include the ratio $\overline{\mathrm{u}}/\overline{\mathrm{d}}$ as measured by NA51 [17], instead of the "GRV LO" set [12] used for the 1995 data analysis reported above. It must be stressed that results in this section are still preliminary and that systematic errors have not yet been evaluated.

4.1. (J/ψ)/(Drell–Yan) ratios

The ratio $B_{\mu\mu}\sigma^{J/\psi}/\sigma^{DY}$ is presented in fig. 9 and in table 2 as a function of E_T for 15 centrality classes, extending to very peripheral interactions; quoted errors are statistical

only. The 1995 data are also reported for comparison; all values are given at the actual beam momentum of 158 GeV/c and there is no isospin correction to the Drell–Yan cross–section.

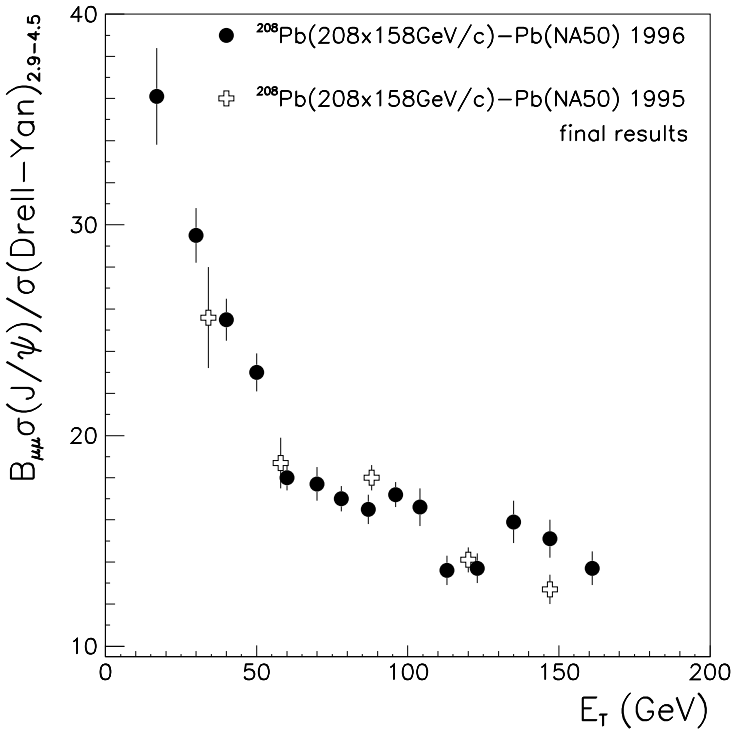

Figure 9. The ratio (J/ψ)/DY vs. E_T at 158 GeV/c (1995 and 1996 data).

There is complete agreement between the two data sets, and the data exhibit a sharp change in the value of the ratio at $E_T \simeq 50$ GeV (where the transverse energy resolution is about 5 GeV). The anomalous J/ψ suppression can now be studied within the Pb–Pb sample itself, without the need of beam energy and isospin corrections which inevitably introduce uncertainties in the analysis.

To confirm that the observed sharp change is really due to an anomalous behaviour of the J/ψ, the number of fitted J/ψ's per GeV is shown in fig. 10 together with the number of opposite–sign dimuons in the relevant mass region $2.9 < M < 3.3$ GeV/c^2, corrected for Drell–Yan contribution. The fitted numbers of J/ψ's per GeV and of Drell–Yan pairs (before acceptance correction) are listed in table 2. Finally, the raw number of dimuons having $M > 4.2$ GeV/c^2 (essentially pure Drell–Yan) is shown in fig. 11. From all this it is clear that the rapid decrease of the ratio at about 50 GeV E_T cannot be due to a discontinuity in the Drell–Yan spectrum (note that the denominator of the

Table 2
The $(J/\psi)/DY$ ratio as a function of E_T (1996 data)

Class	$< E_T >$ (GeV)	$(J/\psi)/DY(2.9-4.5)$ (acceptance corrected)	N_ψ/GeV (fit)	N_{DY}/GeV (fit)
1	17	36.1 ± 2.3	1041	32
2	30	29.5 ± 1.3	1435	54
3	40	25.5 ± 1.0	1583	69
4	50	23.0 ± 0.9	1610	79
5	60	18.0 ± 0.6	1535	95
6	70	17.7 ± 0.8	1560	99
7	78	17.0 ± 0.6	1570	103
8	87	16.5 ± 0.7	1500	102
9	96	17.2 ± 0.6	1477	96
10	104	16.6 ± 0.9	1398	94
11	113	13.6 ± 0.7	1315	107
12	123	13.7 ± 0.7	1225	100
13	135	15.9 ± 1.0	1032	73
14	147	15.1 ± 0.9	970	72
15	161	13.7 ± 0.8	201	16

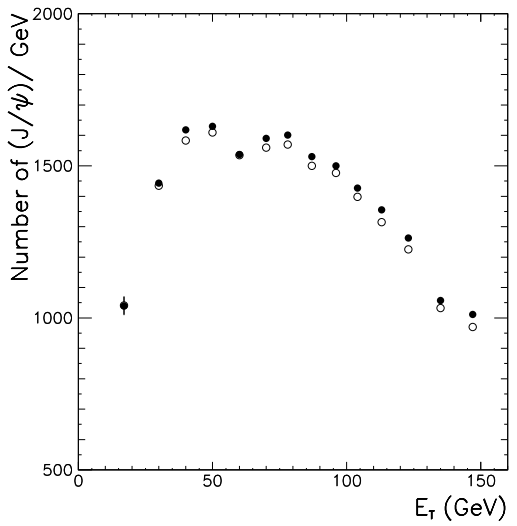

Figure 10. Fitted (open circles) and counted (full circles) number of J/ψ per GeV vs. E_T in Pb–Pb.

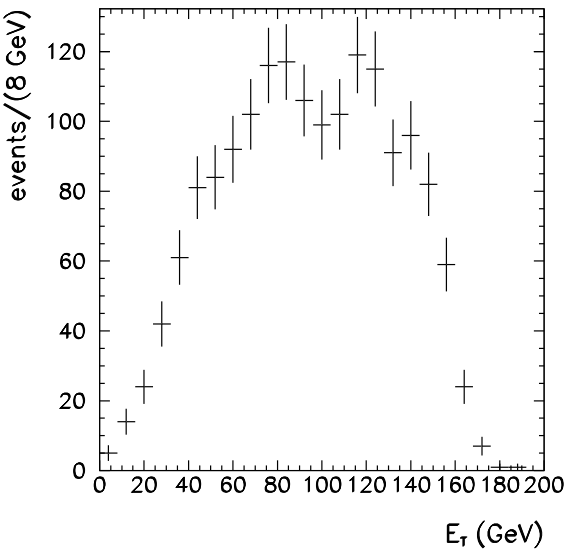

Figure 11. Number of Drell–Yan events ($M >$ 4.2 GeV/c^2) vs. E_T in Pb–Pb.

ratio is computed using Drell–Yan fitted values, which take into account the wider mass region $M > 2.9$ GeV/c^2). On the other hand, more statistics and a full understanding of systematics errors seem to be necessary in the high E_T part of the the Drell–Yan spectrum.

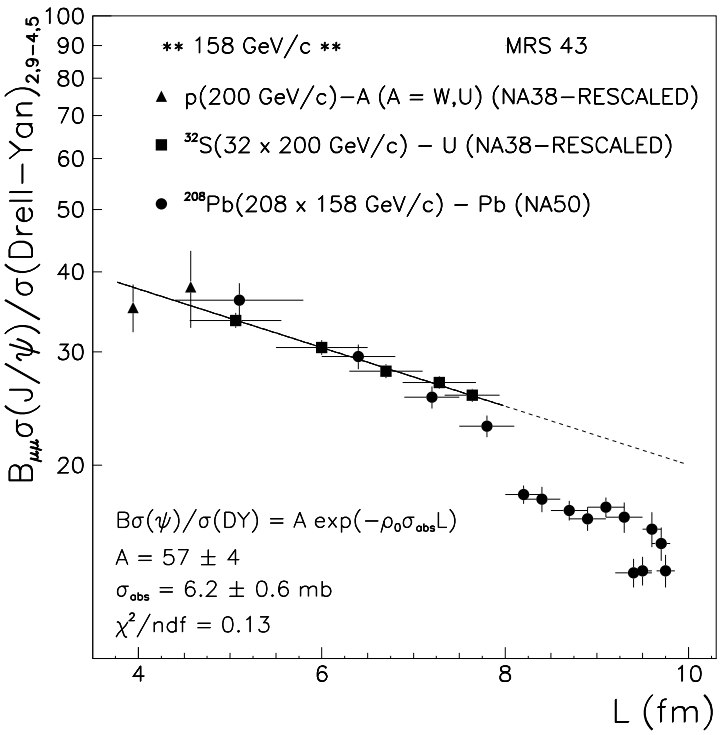

Figure 12. The ratio $(J/\psi)/DY$ vs. L at 158 GeV/c.

Finally, the 1996 Pb–Pb $(J/\psi)/DY$ ratios are compared to previous results (rescaled to 158 GeV/c) in fig. 12, as a function of L. A fit to p–A and S–U data with the absorption model is superimposed. The peripheral Pb–Pb points are essentially compatible with the S–U ones, while a sharp decrease is visible at $L \simeq 8$ fm, suggesting the onset of a new mechanism responsible for the anomalous suppression. The more central points lie almost 10 σ below the absorption line.

4.2. ψ'/(Drell–Yan) ratios

The ratio $\psi'/(DY)$ has been studied as it can provide complementary information on the mechanisms at work for charmonium suppression: the ψ' has a larger radius and a lower threshold for breakup with respect to the J/ψ.

The measured ratios are shown in fig. 13 for proton–nucleus, S–U and Pb–Pb collisions as a function of L. The latter data are reported for 9 centrality classes only because of lower statistics for the ψ'. An absorption model fit has been done to the NA51 and NA38

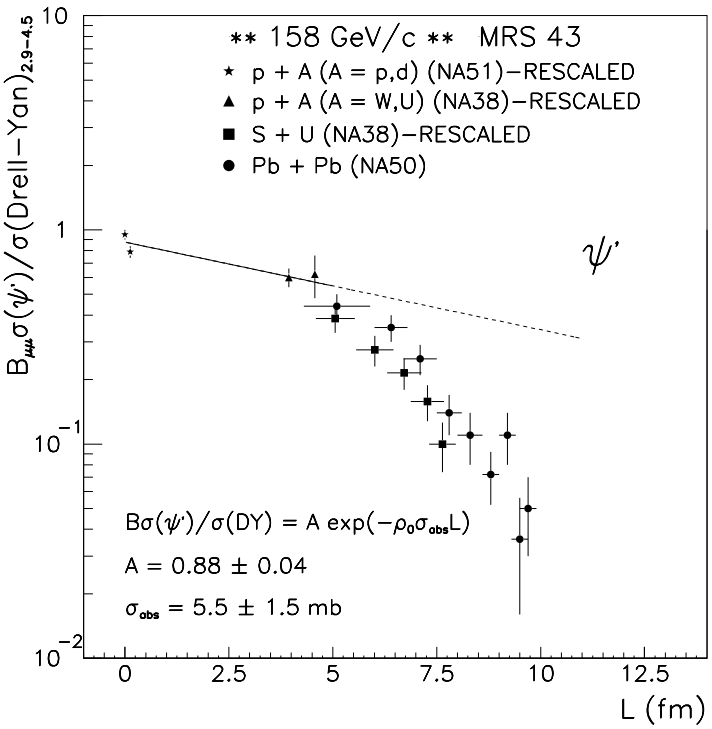

Figure 13. The ratio ψ'/DY vs. L at 158 GeV/c.

p–A data, giving a slightly lower value of absorption cross–section than in the J/ψ case (but compatible within errors).

For the ψ' we observe that both S–U and Pb–Pb data depart from the fit, showing a very similar suppression pattern with respect to Drell–Yan, which appears at much lower L values with respect to the J/ψ. This suggests that a common mechanism for ψ' suppression could be at work in S–U and Pb–Pb collisions.

Absorption by comovers (hadrons produced in the vicinity of the $c\overline{c}$ state) has been proposed by several authors [18–20] as a candidate suppression mechanism both for J/ψ and ψ': our data would indicate that a single mechanism (on top of the established absorption by participant nucleons) cannot explain at the same time the J/ψ and the ψ' suppression patterns.

4.3. Transverse momentum distributions

The p_T distributions of charmonia and of Drell–Yan pairs should provide important information about the nature of the medium formed in heavy ion collisions. Initial state effects (parton multiple scattering before the formation of the $c\overline{c}$ or the Drell–Yan pair) should cause p_T broadening, as already observed in p–A collisions [21], with a magnitude depending on the nature of the partons. The fate of the $c\overline{c}$ should in turn depend on its p_T [22,23].

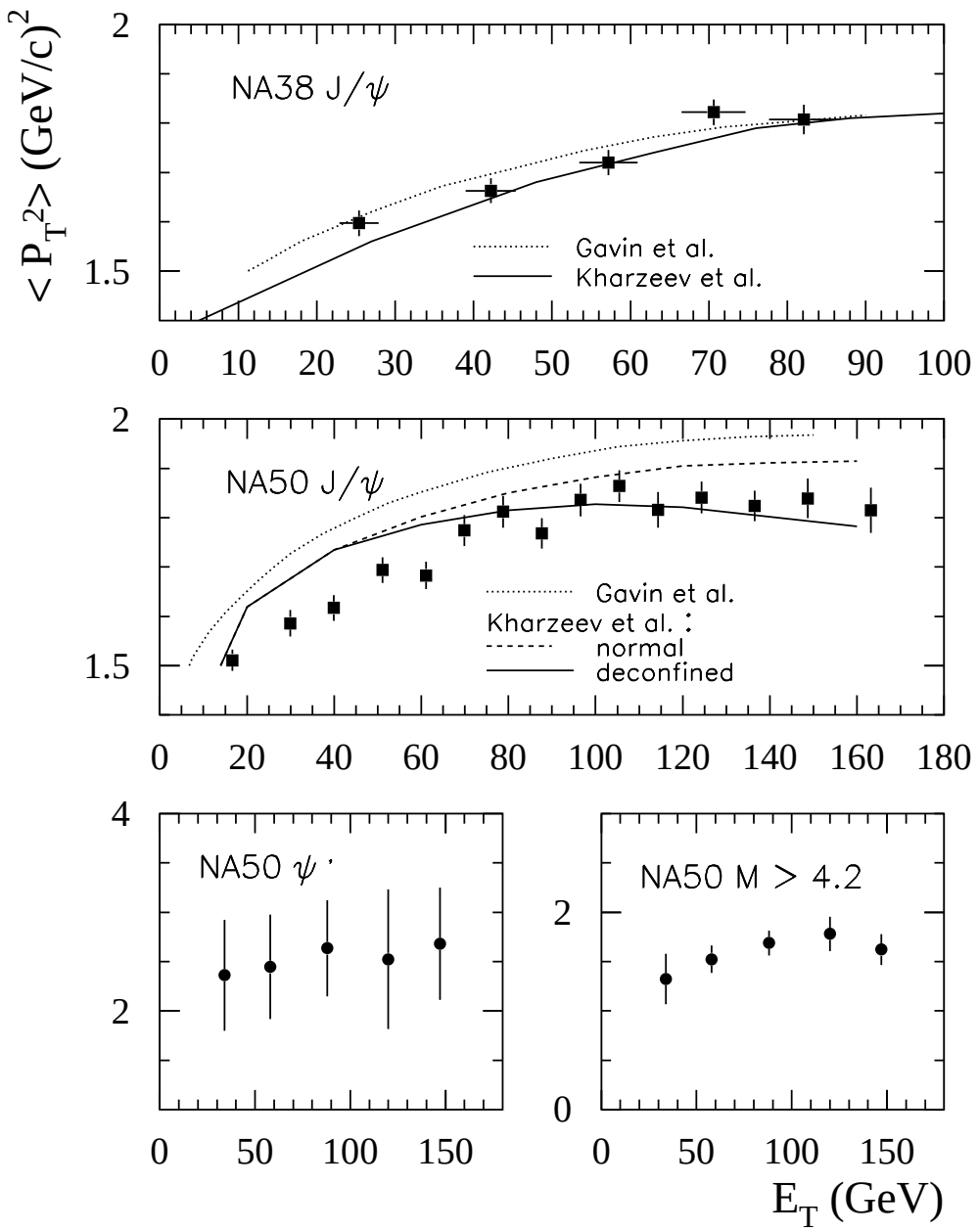

Figure 14. Average p_T^2 vs. E_T for J/ψ in S–U (top) and Pb–Pb (middle), and for ψ' (bottom left) and high–mass Drell–Yan (bottom right) in Pb–Pb.

In order to extract p_T distributions for different dimuon sources, a new 4–dimensional method for acceptance and smearing calculations and for combinatorial background subtraction has been used [24]. The dN/dp_T distributions have been analysed in terms of their moments $< p_T >$ and $< p_T^2 >$. The average p_T^2 of J/ψ is shown in fig. 14 as a function of E_T, for NA38 S–U data and for NA50 Pb–Pb data. The calorimeter coverage was $1.7 \leq \eta_{lab} \leq 4.1$ for NA38. The new analysis of S–U data is compatible within errors with the previous one [25].

The $< p_T^2 >$ of J/ψ in Pb–Pb, after an initial increase with transverse energy, does not increase any more for $E_T \geq 100$ GeV, while in S–U a rather continuous increase with E_T is observed. A change in behaviour is again seen for high E_T Pb–Pb collisions. For comparison, the transverse momentum behaviour observed by NA50 in other mass regions, namely ψ' and high mass Drell–Yan, is presented in fig. 14. The slope of the Drell–Yan $< p_T^2 >$ appears smaller than for the low E_T slope of the J/ψ (a factor of about 2 smaller broadening for quarks compared to gluons is expected from initial state scattering [26]), but clearly more precise Drell–Yan data would be necessary.

On figure 14 two recent predictions for the transverse momentum dependence in Pb–Pb collisions, are reported: the first one [27] predicts a flattening in Pb–Pb (with respect to S–U) using a hadronic comover scenario, while the second one [28] predicts a turn–over and decrease of $< p_T^2 >$ with increasing E_T (curve labelled as "deconfined") because of J/ψ removal from the central part of the interaction region. Both predictions use the available p–p, p–A data and the NA38 S–U data [25] to fix the model parameters.

To investigate further the transverse momentum dependence of J/ψ suppression, the ratios $R_i(P_T)$ between the p_T distribution in a given centrality class and the distribution in the lowest E_T class:

$$R_i(P_T) = \frac{(dN/dP_T)_{ETi}}{(dN/dP_T)_{ET1}}$$

have been formed, each dN/dP_T being normalized to the number of Drell–Yan events in the same E_T class. This analysis has been done in five classes of roughly similar centrality (listed in table 3) for S–U and Pb–Pb data.

Table 3
Centrality classes used for $R(P_T)$ analysis

Class	NA38 $< E_T >$ S–U (GeV)	NA50 $< E_T >$ Pb–Pb (GeV)
ET1	25	34
ET2	42	58
ET3	57	88
ET4	71	120
ET5	82	147

The ratios $R_i(P_T)$ are presented in fig. 15 for S–U and in fig. 16 for Pb–Pb interactions. There is a clear indication for more J/ψ suppression at low p_T, and the ratio for Pb–Pb is

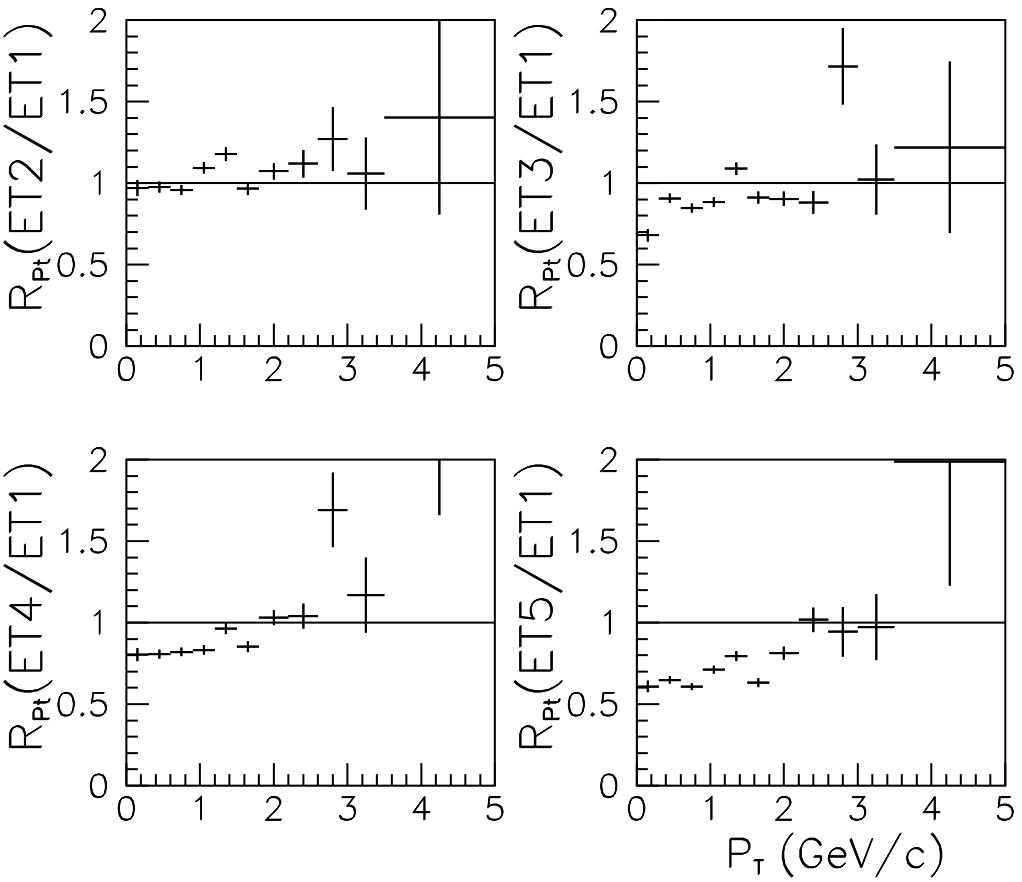

Figure 15. Ratio of p_T distributions of J/ψ in different E_T bins for S–U (NA38) data.

consistently below unity for p_T up to about 2 GeV/c for classes 1–4, showing an approximate saturation at higher p_T. Regarding S–U data, the high p_T points, although with large error bars, are not incompatible with a ratio greater than unity, which would point again to a different suppression mechanism in the two systems.

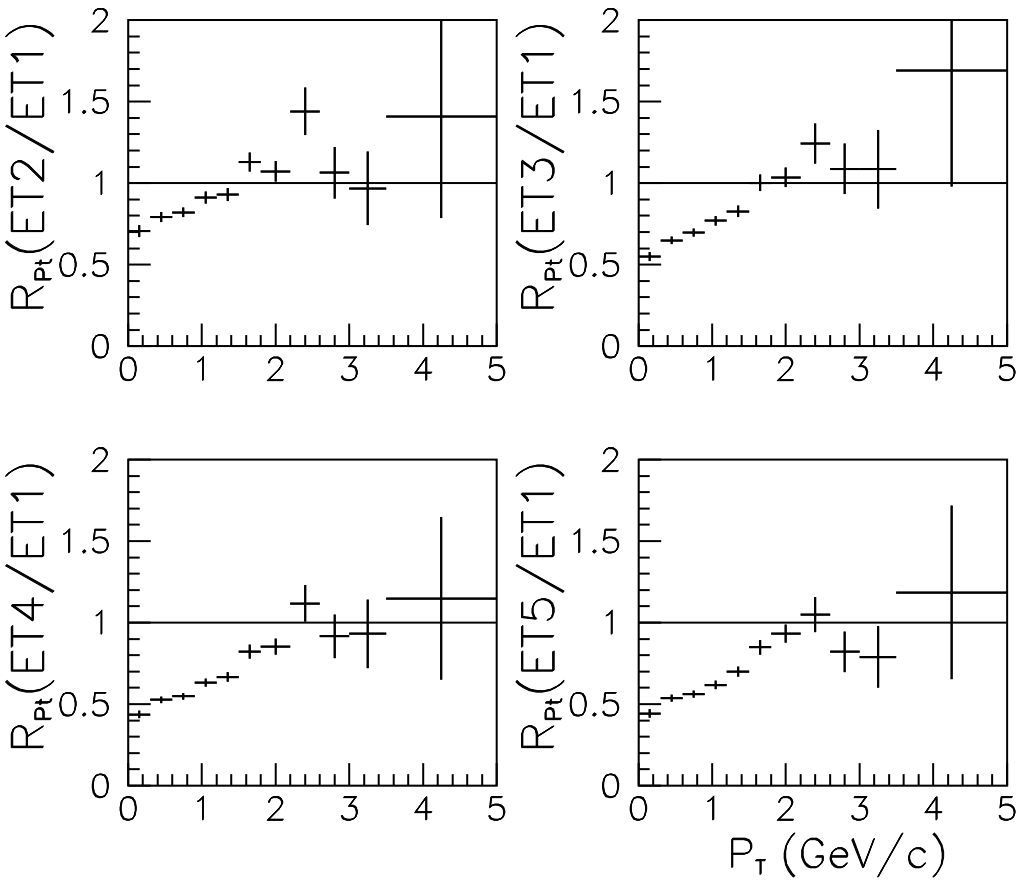

Figure 16. Ratio of p_T distributions of J/ψ in different E_T bins for Pb–Pb (NA50) data.

5. CONCLUSIONS

NA50 has measured charmonium and Drell–Yan production with better statistics and extended centrality range in the 1996 run. The anomalous suppression of J/ψ in Pb–Pb collisions, namely a departure from the ordinary suppression pattern $\sigma^{AB} = \sigma^{NN}(AB)^{\alpha}$ holding from p–p to central S–U collisions, has been confirmed.

The ratio $B_{\mu\mu}\sigma_{J/\psi}/\sigma_{DY}$ shows a strong discontinuity within the Pb–Pb sample at $E_T \simeq 50$ GeV, corresponding to a path $L \simeq 8$ fm. The suppression pattern of ψ' relative to Drell–Yan versus L is very similar in the S–U and Pb–Pb data, pointing to a common mechanism. The $< p_T^2 >$ of J/ψ does not increase any more for $E_T \geq 100$ GeV.

6. Acknowledgements

We are grateful to the CERN SPS team and in particular to Lau Gatignon for their excellent job in providing a high quality beam.

Note added in proof: The statistical errors quoted in figures 7, 8, 9, 12, 13 and in table 2 are underestimated by a factor 1.4 for Pb–Pb data and by a factor 2.8 for S–U data.

REFERENCES

1. T. Matsui and H. Satz, Phys. Lett. B178 (1986) 416.
2. C. Baglin et al., Phys. Lett. B220 (1989) 471; B255 (1991) 459; B270 (1991) 105.
3. M. Gonin et al., NA50 coll., Nucl. Phys. A610 (1996) 404c.
4. M.C. Abreu et al., Phys. Lett. B410 (1997) 327.
5. M.C. Abreu et al., Phys. Lett. B410 (1997) 337.
6. M. Gonin et al., RHIC'97 Summer study, Brookhaven, July 1997.
7. F. Ohlsson–Malek, NA50 coll., HEP '97 EPS Conference, Jerusalem, August 1997.
8. D. Jouan for the NA50 collaboration, contribution to this Conference.
9. A. De Falco for the NA50 collaboration, contribution to this Conference.
10. E. Scomparin et al., NA50 coll., Nucl. Phys. A610 (1996) 331c.
11. M.C. Abreu et al., NA51 collaboration, in preparation.
12. M. Glück et al., Z. Phys. C53 (1992) 127.
13. D.M. Adle et al., Phys. Rev. Lett. 66 (1991) 133.
14. D. Kharzeev and H. Satz, Phys. Lett. B366 (1996) 316.
15. G.A. Schuler, CERN–TH.7170/94 (hep–ph/9403387), 1994.
16. A.D. Martin et al., Phys. Rev. D51 (1995) 4756.
17. A. Baldit et al., NA51 collaboration, Phys. Lett. B332 (1994) 244.
18. S. Gavin and R. Vogt, Nucl. Phys. A610 (1996) 442c.
19. A. Capella et al., Phys. Lett. B393 (1997) 431.
20. W. Cassing and C.M. Ko, Phys. Lett. B396 (1997) 39.
21. J. Badier et al., Z. Phys. C20 (1983) 101.
22. F. Karsch and R. Petronzio, Phys. Lett. B212 (1988) 255.
23. M.C. Chu and T. Matsui, Phys. Rev. D37 (1988) 1851.
24. M.C. Abreu et al., NA38 collaboration, in preparation.
25. C. Baglin et al., Phys. Lett. B262 (1991) 362.
26. Hüfner et al., Phys. Lett. B215 (1988) 218.
27. S. Gavin et al., preprint hep–ph/9610432.
28. D. Kharzeev et al., preprint BI–TP 97/02.